Loose nanofiltration membranes functionalized with in situ-synthesized metal organic framework for water treatment

Loose Nanofiltration Membranes Functionalized With in Situ-Synthesized Metal Organic Framework for Water Treatment

Sina Mohammad Nejad[1+], S. Fatemeh Seyedpour[1,2+], Sadegh Aghapour Aktij[2,3+], Mostafa Dadashi Firouzjaei[4], Mark Elliott[4], Alberto Tiraferri[5], Mohtada Sadrzadeh[*2], Ahmad Rahimpour[1,2*]

[1] Faculty of Chemical Engineering, Babol Noshirvani University of Technology, Shariati Ave., Babol, 47148-71167, Iran
[2] Department of Mechanical Engineering, 10-367 Donadeo Innovation Center for Engineering, Advanced Water Research Lab (AWRL), University of Alberta, Edmonton, AB, Canada, T6G 1H9
[3] Department of Chemical & Materials Engineering, 12-263 Donadeo Innovation Centre for Engineering, University of Alberta, Edmonton, AB, Canada, T6G 1H9
[4] Department of Civil, Construction and Environmental Engineering, University of Alabama, Tuscaloosa, 35487, USA
[5] Department of Environment, Land and Infrastructure Engineering (DIATI), Politecnico di Torino, Corso Duca degli Abruzzi 24, 10129 Turin, Italy

* Corresponding Authors:

Ahmad Rahimpour (arahimpo@ualberta.ca), Mohtada Sadrzadeh (mohtada@ualberta.ca)

[+] These authors contributed equally to this work.

Abstract

In this study, modified loose nanofiltration membranes were prepared by in-situ decoration with ZIF-7 on the surface of porous polyethersulfone substrates functionalized with co-deposited sulfobetaine methacrylate zwitterion (ZW) and polydopamine (PDA). By the aid of ZW/PDA active layer co-deposition under mild conditions, ZIF-7 metal organic framework nanocrystals were successfully formed and anchored onto the membrane surface via both non-covalent and covalent bonds, to simultaneously achieve the desired selectivity and productivity of the loose nanofiltration membranes. The results of characterization confirmed the successful deposition of the ZW/PDA active layer and the consequent decoration with ZIF-7 nanocrystals. The average water contact angle decreased notably from 81.4 to 51.43 degrees upon formation of ZIF-7. This membrane showed high rejection (~99.9%) of either methyl blue and Congo red dyes, and high water flux with dye solutions (around 40 L $m^{-2}h^{-1}$) at very low applied pressure of 1.5 bar. Moreover, the filtration experiments revealed that functionalized membrane exhibited significant reduction in fouling and biofouling propensity.

Keywords: Functionalized membrane, SBMA zwitterion, Co-deposition, dye removal, antifouling, ZIF-7.

Introduction

Dyes are toxic, carcinogenic, and teratogenic substances causing health problems, such as allergy, skin irritation, hard breathing, as well as kidney and liver dysfunction [1]. Dye contaminated wastewaters are a threat to human health and the environment [2] and must be properly treated before discharge into water streams or reuse. Nanofiltration (NF) is desirable in meeting wastewater treatment requirements due to its simple operation, high removal efficiency, low cost and energy consumption [3]. However, fouling is still a severe challenge, resulting in reduced performance and membrane lifetime [4]. For this reason, on of the key ways to successfully deploy NF for wastewater treatment and reuse is the fabrication of membranes with high permeation, rejection, and, importantly, low fouling tendency [5].

Surface modification by hydrophilic polymers, such as polydopamine (PDA), can effectively mitigate fouling [6]. Regarded as a bio-inspired glue, PDA strongly attach to any surface via in-situ self-polymerization of dopamine, forming a highly stable coating [7]. Furthermore, the catechol, quinone, and the amine functional groups on the PDA layer, offer secondary reaction sites for attaching other nanostructures and achieve further functinalization[8]. Membrane surface can thus inherit even higher antifouling properties by additional modification with compounds, such as zwitterions (ZW) and metal-organic frameworks (MOF) [9, 10]. ZW have superior antifouling properties especially capable of reducing protein or bacterial adhesion [11, 12]. The hydration layer formed by ZWs is typically dense, and this feature offers consistent hydrophilicity and fouling control [4]. Furthermore, as a class of MOFs, zeolitic imidazolate frameworks (ZIFs) have outstanding chemical stability and biocidal activity [13]. Considering the hydrophilic nature of both ZWs and ZIFs, their co-deposition with PDA may be a simple method to achieve functionalized antifouling surfaces.

Herein, we develop a method for PDA and sulfobetaine methacrylate (SBMA) co-deposition on porous PES supports under mild conditions. The presence of functional groups on the surface of PDA and ZW is anticipated to enhance dye rejection via electrostatic interaction. Besides, PDA coating provides abundant active sites for the nucleation and growth of ZIF-7 crystals to further functionalize the membrane surface and achieve further antifouling properties, herein investigated. All the membranes are comprehensively characterized, and their performance is evaluated under loose NF conditins for the removal of methyl blue (MB) and Congo red (CR) from aqueous solutions.

Materials and Methods

Reagents. Polyethersulfone (PES, Ultrason E6020P, M_W = 58,000 g/mol) as polymer, N,N-dimethylformamide (DMF, 99.5%, Scharlau) as solvent, Triton X-100 (Merck) and polyvinyl pyrrolidone (PVP, M_W = 25,000 g/mol, Merck) as pore formers, were used for preparation of porous substrate casting solutions. Dopamine hydrochloride (DP, 98%, Merck), Trizma hydrochloride (Trizma-HCl, Merck), sulfobetaine methacrylate (SBMA, M_W = 279.36 g/mol, Merck), and phosphate-buffered saline (PBS) were purchased from Sigma Aldrich. $Zn(NO_3)_2.6H_2O$ (≥ 98.0 %, Merck) and benzimidazole (≥ 98.0 %, Merck) were used for the synthesis of ZIF-7 crystals. Methyl blue (MB, Merck) and Congo red (CR, Merck) were selected as model anionic dyes. Sodium alginate was purchased from Sigma-Aldrich. Potassium dihydrogen phosphate (KH_2PO_4, 99.5%), glucose monohydrate, magnesium sulfate ($MgSO_4.6H_2O$, 99%), sodium bicarbonate ($NaHCO_3$, 99.5%), calcium chloride ($CaCl_2$, 96%), and ammonium chloride (NH_4Cl, 99.5%) purchased from Merck were used for the preparation of the synthetic wastewater.

Fabrication of ZIF-7 Functionalized NF Membranes. The porous PES support membrane was fabricated via non-solvent induced phase inversion by immersion precipitation technique (denoted as blank membrane hereafter).[14] The PDA self-polymerization on the membrane surface was performed by preparing 2.0 g/L DA in Tris (pH = 8.5, 0.089 M). The fixed blank membrane was soaked in DA solution with the active side facing the solution for 2 h at room temperature while shaking to provide sufficient oxygen for PDA formation. The PDA coated membranes were thoroughly rinsed with deionized (DI) water and stored overnight in DI water to remove unattached monomers (denoted as PDA membrane). To form ZIF-7 in-situ, the PDA membrane was immersed in a metallic aqueous solution containing 0.446 g of $Zn(NO_3)_2 \cdot 6H_2O$ in 100 mL deionized water for 45 min. After removing the excess metallic solution, the Zn anchored membrane was soaked in the benzimidazole solution containing 0.354 g in 100 mL of ethanol for 30 min at ambient temperature. Finally, this ZIF-7 functionalized membrane (denoted as MOF-PDA membrane) was washed with DI water and dried at room temperature. Both metallic and linker solutions were sonicated for 5 min before use to remove any aggregation.

To tailor the functionalization of ZIF-7, other membranes (labeled as MOF-SBMA/PDA) were obtained via co-deposition of PDA/SBMA on the PES support layer. Specifically, 1 g/L SBMA was incorporated into the 1 g/L DA solution and all the steps for fabrication of PDA membrane were repeated. Then, the SBMA/PDA coated membrane was subjected to the same sequential steps of ZIF-7 functionalization described above for the MOF-PDA membrane. Therefore, the membranes investigated in this study include: (i) blank membrane (PES porous support); (ii) PDA membrane; (iii) MOF-PDA membrane; and (iv) MOF-SBMA/PDA membrane. **Figure 1** illustrates the step-by-step procedures of membrane functionalization.

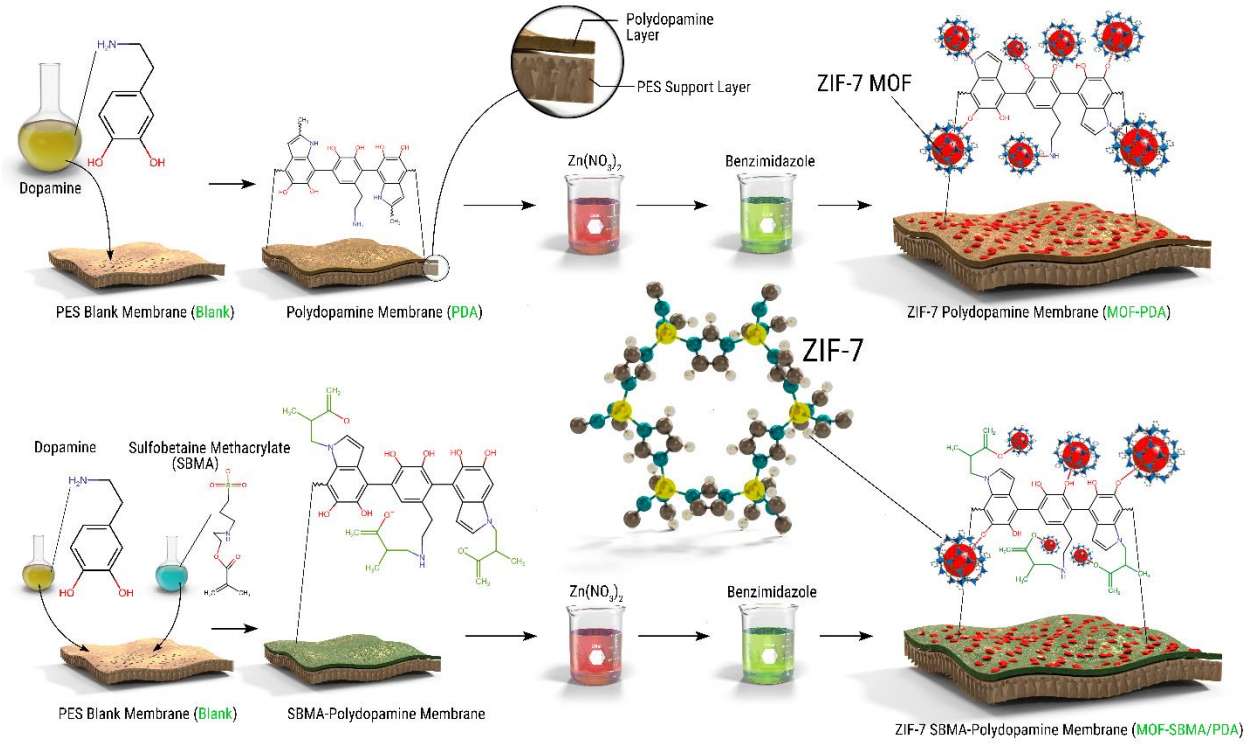

Figure 1. Illustration of membrane functionalization procedures including: blank membrane; PDA coated membrane (PDA membrane); MOF depositition on PDA coated membrane (MOF-PDA membrane); MOFdeposition on SBMA/PDA coated membrane (MOF-SBMA/PDA membrane).

Membrane Surface Characterization. Field emission scanning electron microscopy (FE-SEM, MIRA3 TESCAN) coupled with energy-dispersive X-ray Spectrometer (EDX) was used to characterize both the membrane top surface and the membrane cross-sectional morphologies. The cross-section morphology was further investigated by transmission electron microscopy (TEM, JEOL JEM-ARM200CF), operated at 20 kV. Atomic force microscopy (AFM, EasyScan II, Swiss) was applied to determine the surface roughness of membrane samples. To minimize the experimental error, the surface roughness was determned for three separate samples of each membrane type. Fourier transform infrared spectroscopy (FTIR, Thermo Scientific USA) was used to identify the functional groups of the anchored membrane. The surface electric potential of all membranes was evaluated with an Anton Paar SurPASS electrokinetic solid surface potential analyzer (Anton Paar USA, Ashland, VA). All the streaming potential measurements

were conducted in a background electrolyte solution composed of 1 mM KCl at 25 °C, over a pH 4–9 range. The zeta potentials were calculated based on the Helmholtz-Smoluchowski equation. Two separate samples for each membrane type were assessed to assess repeatability. The membrane surface hydrophilicity was evaluated by means of contact angle (CA) measurements (Dataphysics, OCA 15 plus), where an average value of five random positions were probed to calculate a meaningful average. The elemental composition and chemical features of the membrane surfaces were evaluated with X-ray photoelectron spectroscopy (XPS, Bestec, Germany).

Membrane Transport and Fouling Evaluation. The flux and dye rejections of the membranes were evaluated at an operating pressure of 1.5 bar with a dead-end cell and with an effective membrane surface area of 30 cm^2. MB and CR were selected as model anionic dyes[15]. Further information on the dead-end setup and the performance evaluation are explained in **SI.1.1**. The organic fouling and bio-fouling propensity of the membranes were assessed with feed solutions containing humic acid and *E. coli* (model bacteria), respectively, guided by our previous studies (further detail on dynamic fouling experiments is provided in **SI.1.2**).[16]

Metal ion Release Rate. The release rate of zinc ions from the membranes was evaluated via batch experiments. Briefly, MOF-PDA and MOF-SBMA/PDA membranes coupons (1 cm^2) were separately immersed in 60 mL of DI water and then placed on an orbital shaker (100 rpm) for several days and the water was replaced every 24 h. Aliquots were taken and acidified using HNO_3 and then analyzed by inductively coupled plasma optical emission spectrometry to determine their Zn content.

Results and Discussions

Physiochemical properties of the membranes. The catechol moiety of PDA enhanced the connection between the PES substrate and grafted SBMA or anchored ZIF-7. As illustrated in **Figure 1**, a two-step surface modification occurs for MOF-SBMA/PDA membranes, in which (i) a thin layer of PDA and SMBA was initially co-deposited on the membrane surface, and (ii) ZIF-7 nanocrystals were in-situ attached on the active sites of this layer. Since SBMA has methacrylate functional groups, it undergoes an aza-Michael reaction with PDA amine groups. As a result, the nucleophilic amines of PDA connected to electron-withdrawing α, β-unsaturated carbonyl moieties [17]. Due to the presence of water molecules, hydrogen bonds form, which promote the aza-Michael reaction by increasing the electrophilic trait of carbon and the nucleophilic feature of the nitrogen atom in the amine (**Figure SI.1)**. Co-deposition of SBMA/PDA is expected to facilitate post-modification of membrane with ZIF-7 crystals and improve the stability of the coating. The dopamine monomers act as bio-glue and their amine groups react with methacrylates moieties of SBMA to attain covalently grafting. Meanwhile, PDA regulates the nucleation and growth sites and this results in robust coordination interactions and therefore rapid bio-functionalization of ZIF-7 on the surface.[18] It has been well established that the catechol groups present on PDA surface chelate various metal ions.[19-23] The ensuing Zn ions served as seeds that eventually grew into spherical ZIF-7 nanostructures after introducing the benzimidazole ligand.[24, 25] In other words, the nucleated Zn ions coordinated with the −NH functional moieties of benzimidazole ligand and formed stable ZIF-7 nanocrystal ZIF-7 on SBMA/PDA substrate.[26-28]

The FTIR spectroscopy was conducted to distinguish the functional groups of membrane surface and to confirm the successful deposition of PDA and ZIF-7 nanocrystal on the substrate

(**Figure 2**). Peaks appeared at around 1150 and 1240 cm^{-1}, corresponding to the symmetric O=S=O stretching vibration of the sulfone group and asymmetric C–O–C stretching vibration of the aryl ether group of the blank membrane, respectively.[29] The peaks observed at around 1300, and 1320 cm^{-1} may be assigned to the doublet from the asymmetric O=S=O stretching vibration.[29] The band at around 1485 cm^{-1} corresponds to the C–C stretching vibrations in the aromatic ring.[30, 31] Furthermore, the absorption band observed at about 740 cm^{-1} may be attributed to the out-of-plane C–H bending vibration of ortho-disubstituted benzene present in benzimidazole ligand of the ZIF-7, which is in accordance with previously reported studies. [32] Comparing the spectra of all membranes, a new peak emerged at 759 cm^{-1} for MOF-PDA and MOF-SBMA/PDA membranes, which corresponds to the ZIF-7, corroborating the formation of the ZIF-7 nanocrystals on the membranes surface.[5] The benzimidazole ligand displays several N-H signals between 3300 and 2500 cm^{-1} (Aldrich Library of FTIR spectra, ed II, vol. 3), however, many of these peaks disappeared after the coordination with Zn atoms, representative of ZIF-7 formation.[33, 34] The stretching vibrations of MOF-PDA and MOF-SBMA/PDA membranes at around 916 cm^{-1} may be ascribed to the Zn–OH bond, confirming the decoration of Zn atoms on the catechol groups of PDA. [8, 9] Meanwhile, a peak at around 997 cm^{-1} may be attributed to the C-N stretching vibration of the ZIF-7 structure. [10]

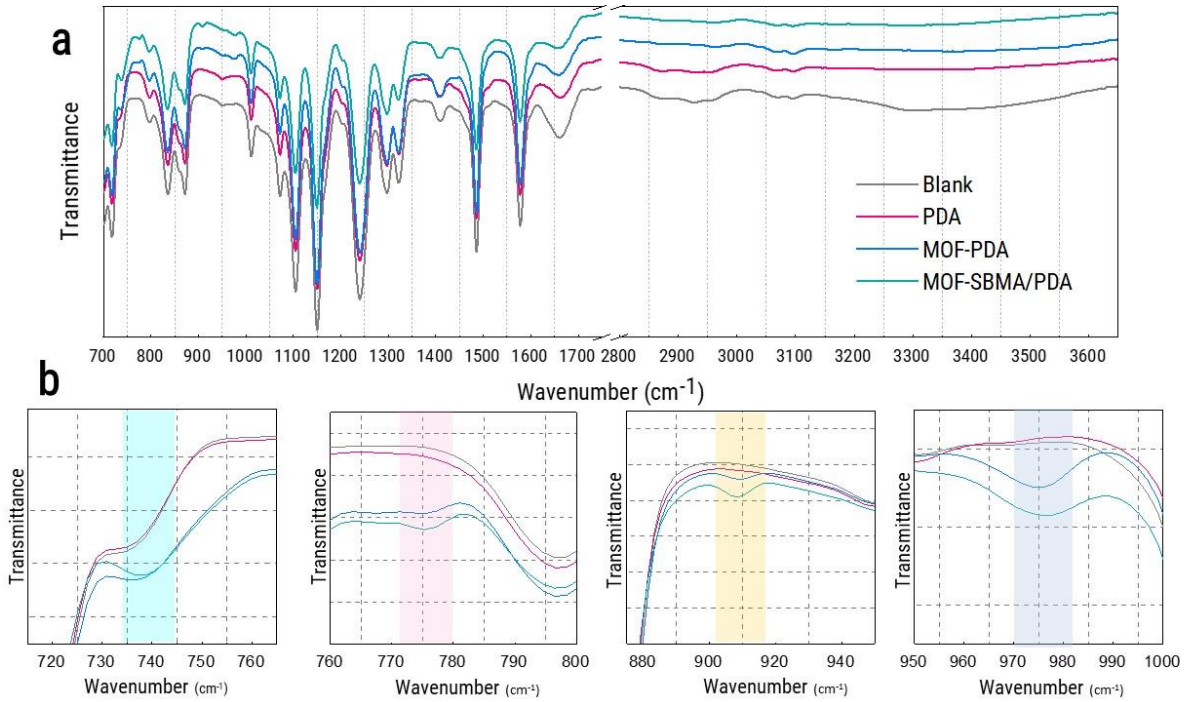

Figure 2FITR spectra of blank and modified membranes: (a) survey, and (b) high-resolution spectra.

The elemental composition and chemical structure of blank and modified membranes were evaluated by XPS analysis with results shown in **Figure 3**. The survey spectra of all membranes mainly comprise the energy peaks of carbon (C), nitrogen (N), oxygen (O), and sulfur (S) atoms, located at 284.5, 399, 532, and 168.6 eV, respectively. However, appearance of two new Zn signals located at 1021.3 and 1044.4 eV (attributed to Zn $2p_{3/2}$ and $2p_{1/2}$, respectively) indicate the presence of ZIF-7 nanocrystals on the surface of both ZIF-7 decorated membranes (MOF-PDA and MOF-SBMA/PDA).[38, 39] The elemental compositions of blank and modified membranes are presented in **Table 1**. N atoms on the blank membrane are attributed to the presence of PVP in the support layer. After PDA deposition, the content of N atoms decreased slightly and then increased significantly after ZIF-7 decoration. [40] The negligible reduction of N and slight increment of S atoms in MOF-SBMA/PDA membrane can be referred to the incorporation of SBMA to the PDA structure.

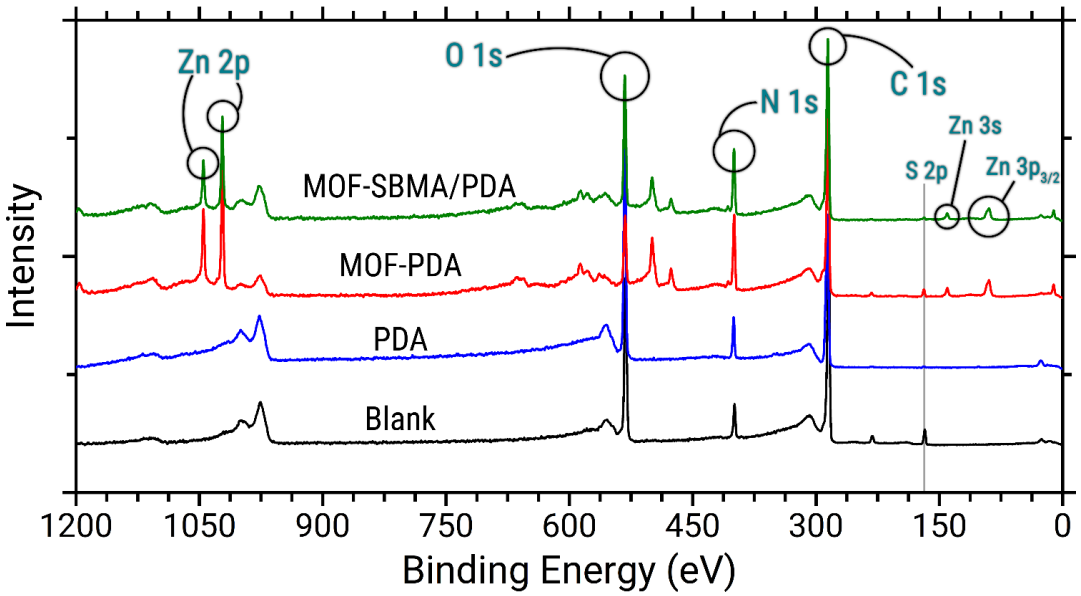

Figure 3. The XPS survey spectra of blank and modified membranes.

Table 1. Elemental compositions of blank and modified membranes.

Membrane	Atomic concentration (%)				
	C(1s)	O(1s)	N(1s)	Zn(2p)	S(2p)
Blank	60.2	30.30	6.80	-	2.70
PDA	69.9	22.00	5.90	-	2.20
MOF-PDA	70.90	9.30	13.20	5.50	1.10
MOF-SBMA/PDA	66.50	16.90	12.00	3.30	1.30

Further information on the chemical structure of membranes and coordination of the ZIF-7 nanoscrystals was obtained by the deconvolution of the C1s and N1s high-resolution spectra (**Figure SI.2**). Regarding the blank membrane containing PVP as additive, the de-convoluted spectrum of C 1s reveals C=C, C–C/C–H, C–N/C–O/C–S, and O=C–NH bonds located at binding energies of 284.5, 285.9, 287.4, and 288.2 eV, respectively. [39] Due to presence of PVP as additive, the de-convoluted N 1s spectrum represents the –NH– and N^+ bonds at 400.6 and 401.9 eV. The de-convoluted C 1s spectrum of PDA and MOF-PDA membranes showed three main peaks, including C–C/C–H, C–N/C–O, and C=O bonds located at binding energies of 284.5,

285.7, and 287.1 eV, respectively. [18, 41] Besides, the de-convoluted N 1s spectrum of PDA coated membrane showed the =N–C, C–N–C, and N–C bonds located at 398.8, 399.9, and 400.7 eV, respectively. The de-convoluted C 1s spectrum of MOF-SBMA/PDA membrane revealed C=C, C–C/C–H, C–N/C–O/C–S, and C=N/C=O bonds located at binding energies of 284.5, 285.7, 287.3 eV, and 287.9 eV respectively. [39] In case of both ZIF-7 modified membranes, owing to the presence of benzimidazole ligand, three kinds of N-containing functional groups can be observed in the deconvoluted spectrum of N1s, including pyridinic (=N– bond), pyrolic (–NH– bond), and quaternary N centers, located at 398.5, 399, and 400.4 eV, respectively.[34, 42] After reacting with Zn atoms, signal appears that may be associated to the protonated N atoms coordinated with Zn.[42, 43]

The surface and cross section morphologies of all membranes were assessed by FE-SEM and TEM (**Figure 4**). SEM micrographs show relatively smooth surfaces for the PDA membrane, while all the ZIF-7 decorated membranes were characterized by a rougher surface, comprising some PDA aggregates and ZIF-7 nanocrystals on the surface. PDA catechol functional groups can provide anchor sites to react with positively charged Zn ions of ZIF-7 nanocrystals. For this reason, some semi-spherical ZIF-7 nanocrystals were formed on the surface in both cases, for MOF-PDA and MOF-SBMA/PDA membranes. [25] Compared to the MOF-PDA membrane, the quantity of ZIF-7 increased significantly on the MOF-SBMA/PDA membrane, although the surface distribution seems to be heterogeneous in both cases.

A thicker active layer can be observed on the surface of PDA coated membranes, together with a denser upper portion of the support, compared to the blank membrane (**Figure 4 f-h**). Other than forming a surface PDA layer, it is likely that dopamine monomers penetrated into the surface and partly blocked the pores upon polymerization.[37] The SEM micrographs (Figure 4g

vs. 4h) suggest that the clogging degree of the MOF-SBMA/PDA membrane was higher than PDA and MOF-PDA membranes. This phenomenon may be attributed to the co-deposition of PDA/SBMA, which would produce a denser structure as chain entanglement occurs. When a denser structure forms on the surface, it also offers more active sites and functional groups for further functionalization, thus allowing a larger quantity of ZIF-7 nanocrystals to form on the surface, as indicated by the SEM micrographs (Figure 4c vs. 4d).

The corresponding EDX mapping (**Figure SI.2**) of ZIF-7 decorated membranes indeed revealed the presence of Zn ions and nitrogen atoms on the surface. The content of Zn increased on the MOF-SBMA/PDA membrane compared to MOF-PDA, consistent with SEM images. Supporting the aforementioned statements, TEM images (**Figure 4i-l** and **Figure SI.4 , 4**) illustrate that the surface of blank membrane was successfully modified as ZIF-7 nanocrystals formed on the MOF-PDA and, even more importantly, on MOF-SBMA/PDA membrane surface due to the accessibility of a larger density of functional groups.

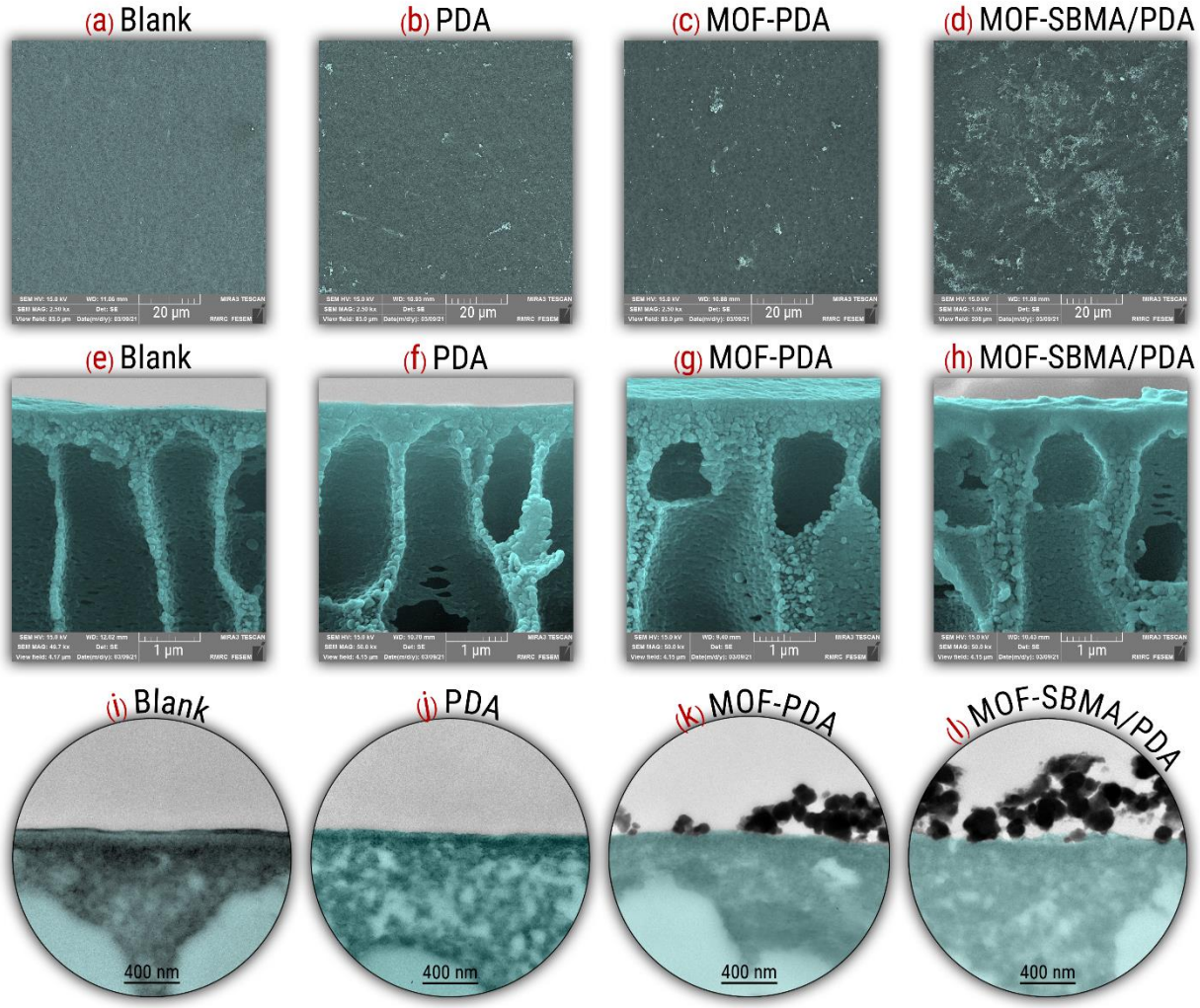

Figure 4. (a-d) the surface FE-SEM images, (e-h) the cross sectional FE-SEM images and (i-l) TEM images of the blank and modified membranes.

AFM images of membrane surfaces and their relevant roughness parameters are illustrated in **Figure 5a-d and Table 2**, respectively. The average roughness of the membrane decreased from 45.32 to 28.81 nm after PDA deposition, indicating appropriate surface coverage. Due to formation of some ZIF-7 nanocrystals on the surface of PDA membrane, the surface roughness of the MOF-PDA membrane increased to 39.59 nm. However, the MOF-SBMA/PDA membrane demonstrated the roughest surface among all membranes as the density and quantity of decorated ZIF-7 nanocrystals increased, consistent with both TEM and FE-SEM images. Even though it is

generally accepted that a rougher membrane is more inclined to fouling and especially biofouling, there is a complex relationship between surface morphological, chemistry and hydrophilicity, and fouling tendency. [45]

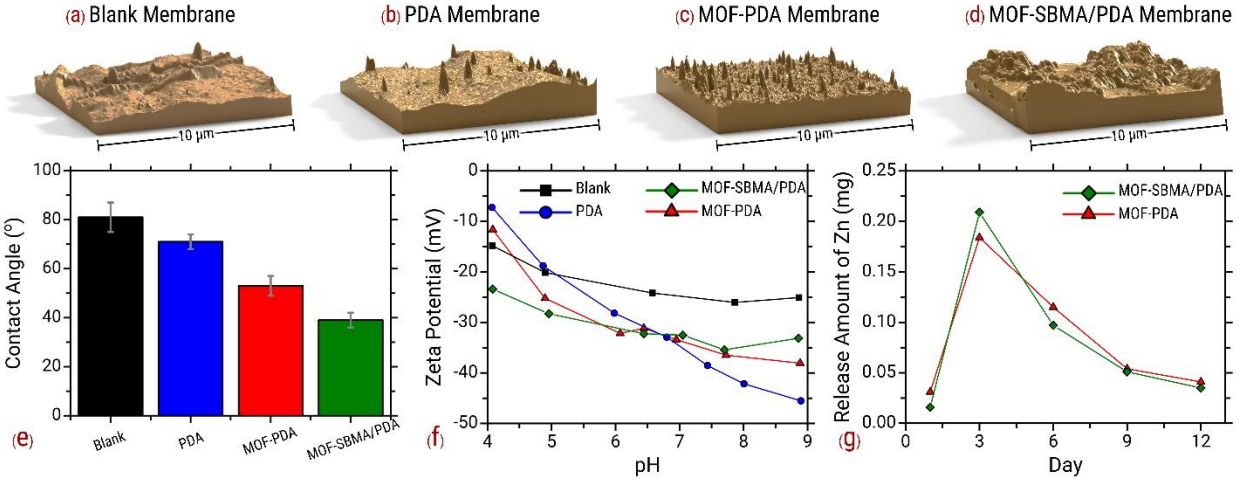

Figure 5. (a-d) surface AFM images, (e) CA, (f) zeta potential and (g) release rate of the blank and modified membranes.

Table 2. Roughness parameters of membranes.

Membrane type	Roughness parameters (nm)	
	Average roughness (R_a)	Root mean squared roughness (R_{rms})
Blank	45.32	58.37
PDA	28.81	38.18
MOF-PDA	39.59	52.65
MOF-SBMA/PDA	238.50	291.50

To evaluate the surface hydrophilicity of the blank and modified membranes, the CA analysis was carried out and the results are depicted **in Figure 5e**. The average CA declined noticeably from 81.4° for the blank membrane to 71.4°, 56.6 °, and 51.43 for PDA, MOF-PDA, MOF-SBMA/PDA membranes, respectively. This descending trend indeed suggests enhanced surface wettability and higher affinity to water molecules. The hydrophilic functional groups of PDA as well as the sulfonate terminals on the SBMA structure (in case of MOF-SBMA/PDA membrane), may be regarded as water acceptor sites and could considerably increase the

hydrophilicity of modified membranes. Generally speaking, this increased surface hydrophilicity is expected to hinder foulant attachment and therefore fouling propensity.[46] When a feed solution contains charged foulants, also surface charge plays an important role in reducing the fouling propensity.[4849, 50] As illustrated in **Figure 5f**, all membranes demonstrated negative zeta potential over the pH range 4–9. Overall, the MOF-SBMA/PDA membrane showed the lowest surface charge at acidic pH, suggesting the presence of moieties undergoing acid-base reaction at highly acidic pH, hence the lowest isoeletric potential (although this value was not attained in the range of pH investigated in this study). The surface potential of this membrane was uniform at basic pH, a behavior usually observed for hydrophilic surfaces that do not adorb hydroxyl ions at increasing pH values. On the other hand, PDA membrane had the higher IEP, a steeper potential curve as a function of pH and the greatest negative charge among all membranes at basic pH values. This behavior is indicative of a combination of different functional groups, protonating and deprotonating at different pH values, consistent with the nature of dopamine monomers.[51, 5253] MOF-PDA membranes showed an intermediate behavior between PDA and MOF-SBMA/PDA membranes, consistent with their surface nature. Generally, a membrane with negatively charge surface is less prone to bacterial deposition and hence biofouling in normal pH ranges[54], as bacterial cells carry negative charges in a pH ranges of 4–9.[55, 56]

Since the stability of decorated ZIF-7 and the controlled release of zinc ions considerably affects the performance and anti-biofouling properties of the modified membranes, zinc leakage assessment was conducted. As displayed in **Figure 5g**, both MOF-PDA and MOF-SBMA/PDA membranes demonstrated the same release trend of zinc ions, which included a rapid rate for the first 3 days and then gradually lowering rate along the subsequent 3-day periods. The initial relatively high zinc release may be ascribed to the release of loosely bound zinc from the surface.

In case of the MOF-SBMA/PDA membranes, the observed slightly higher release rate is rationalized with the higher densityt of deposited ZIF-7. The total leakage rate of zinc ion was low in both membranes and reached a negligible level at the end of the assessing process.[14, 57]

Filtration performance and fouling evaluation of membranes. The separation performance of blank and modified membranes in terms of water flux and dye rejection is presented in **Figure 6**. The water flux of MOF-PDA membrane was significantly lower compared to that of the PDA membrane, namely, it decreased from 78.6 to 28.3 and from 75.3 to 25.6 LMH for CR and MB solutions, respectively. According to the permeability-selectivity trade-off, the dye removal rate by the MOF-PDA membrane increased, from 52 to 94% for CR and from 55 to 96% for MB, resepectively. This behavior indicates that an effective selective layer was formed on the membrane surface via PDA deposition followed by decoration of ZIF-7 nanocrystals.[28] Although the formation of ZIF-7 nanocrystals on the PDA layer sacrificed some membrane flux, it significantly improved dye rejection.

Intrestingly, the water permeability of MOF-SBMA/PDA membrane was notably higher than that observed with the membrane that did not contain zwitterions ((MOF-PDA),with an increment from 28.3 LMH to 41.5 LMH for the CR solution as a feed. At the same time, the rejection performance of this membrane also increased remarkably up to 99.9% for both dyes, attributed to the formation of a denser selective layer, as supported by SEM and TEM images. Although the formation of ZIF-7 on the surface can diminish the water flux, the combination of SBMA with PDA appears to have enhanced the permeability to water as well. SBMA can slow down the PDA polymerization via Michael addition, resulting in a more hydrophilic surface, therefore facilitating water molecules transport (**Figure 5e**). [28] The functional groups present on the PDA chain and SBMA structure may improve dye rejection owing to the charge adjustment

of the composite surface by multiple interactions.[58] In fact, some hydrogen bond, electrostatic, and π-π interactions can be formed due to the existence of amino, imine, and catechol moieties on PDA chain that can increase the selective adsorption performance of the outmost layer .[59, 60] It remains to be determined whether this performance can be maintained also for long term filtrations.

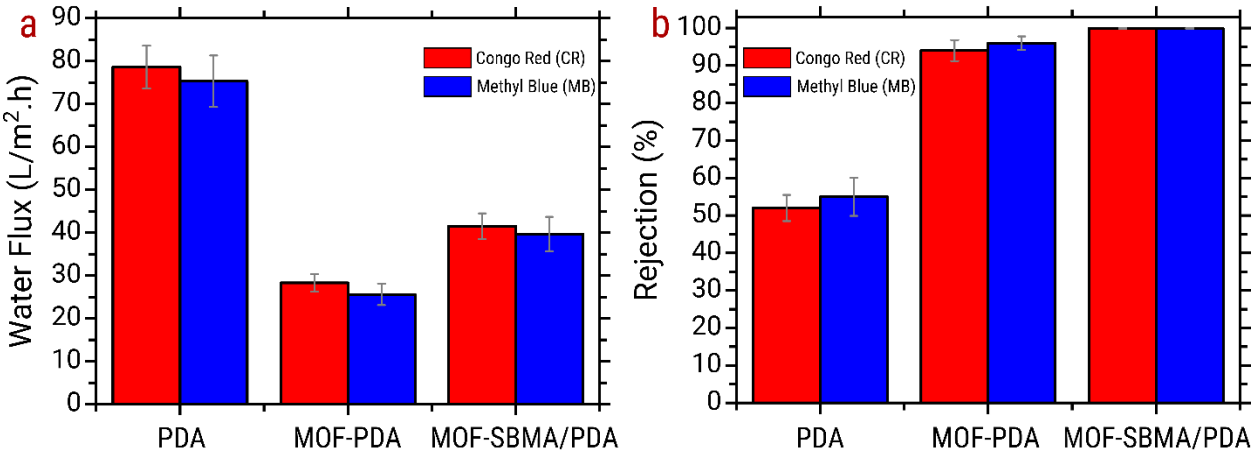

Figure 6. (a) Water flux and (b) dye rejection of blank and modified membranes (ΔP=1.5 bar).

Figure 7 illustrates the results of both organic and biofouling assessment of PDA, MOF-PDA, and MOF-SBMA/PDA membranes, as well also their correspondent flux recovery ratios. The flux declined sharply in the first phase of all fouling experiments, and this phenomenon was particularly important for the PDA membrane. The results summarized in **Figure 7a** indicate a lower rate of flux decline for the MOF-SBMA/PDA in the presence of humic acid. Moreover, as illustrated in **Figure 7b**, after a simple water washing process conducted for 30 min, flux recovery ratios (FRR) of 16.8, 40.4, and 60.3% were achieved for PDA, MOF-PDA, and MOF-SBMA/PDA membranes, respectively. This interesting antifouling properties of the MOF-SBMA/PDA membrane is attributed to the weaker adhesion of humic acid molecules to the hydrophilic surface of this membrane.[61] Furthermore, the nitrogen and oxygen atoms of ZIF-7

nancrystals can also attract water molecules as hydrogen acceptors and form a hydration layer to hamper the humic acid deposition.[62]

The results of biofouling experiments are illustrated in **Figure 7c**. The water flux of PDA membrane declined after introducing of *E. coli* to the feed solution, while the antifouling tendency of modified MOF-PDA, and MOF-SBMA/PDA membranes improved significantly via ZIF-7 formation and/or SBMA co-deposition. In addition, after physical cleaning (**Figure 7d**), FRR of 9.7, 37.9, and 47% were attained for PDA, MOF-PDA, MOF-SBMA/PDA membranes, respectively. This FRR value are consistent with the antibacterial activity of ZIF-7 nanocrystals, which hinder biofilm formation. SBMA structures tend to prevent microbial attachment on membrane surface but they are unsuccessful in deactivating bacteria cells. [65, 66] Therefore, an integration of passive anti-adhesion (SBMA) and active antibacterial (ZIF-7) strategies can result in synergetic effects. [67 68] In addition, the protonated amine groups possibly trigger additional antibacterial property, as they result in cell lysis when in contact with the bacteria [69].

In order to also elucidate the effect of the dye fouling, the flux decline was investigated in the presence of CR for ~24 h (**Figure 7e),** which again revealed the lower fouling tendency for both MOF modified membranes compared to PDA membrane. FRR of 15, 44, and 58% were achieved for PDA, MOF-PDA and MOF-SBMA/PDA membranes, respectively (**Figure 7f)**. The remarkable antifouling properties of both MOF-PDA and MOF-SBMA/PDA compared to that of the PDA membrane may be attributed to their enhanced hydrophilicity and highly negatively charged surfaces.

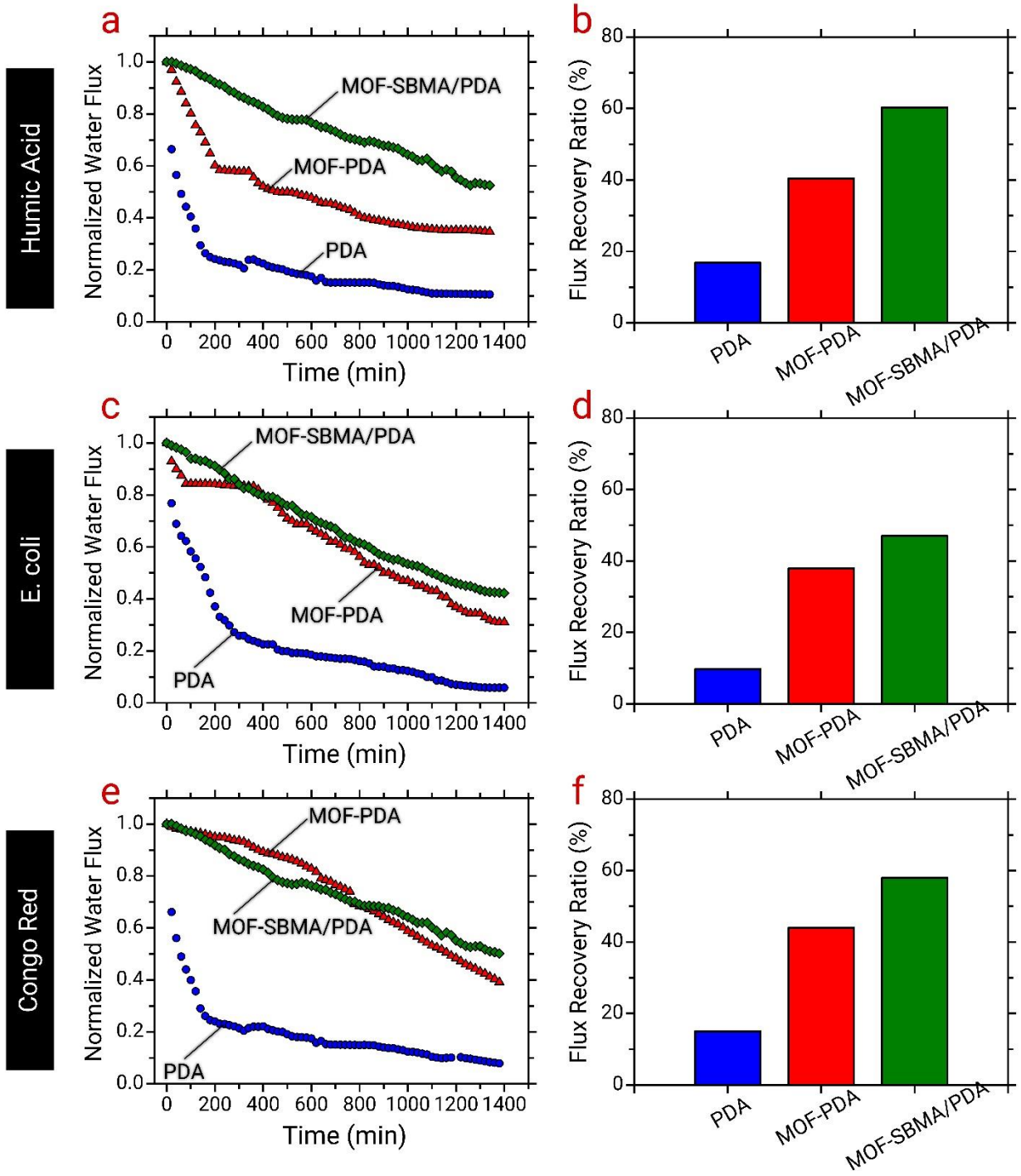

Figure 7. Long-term antifouling performance of the PDA, MMOF-PDA, and MOF-SBMA/PDA membranes versus time.

Table 3 presents a summary comparison between the most performing membrane in this study, namely, MOF-SBMA/PDA, and some membranes developed for dye removal reported in

366 the literature. The productivity (normalized by applied pressure) is one of the highest for our
367 membrane, which showed. comparable separation performance in terms of dye rejection with the
368 membranes previously discussed in the literature. Notably, the MOF-SBMA/PDA membrane
369 displayed favorable antifouling behavior associated with a significant ability to recover flux upon
370 simple physical cleaning. The combination of these two properties is possibly the most
371 promising feature of the membrane proposed in this study.

Membrane type	Membrane Support layer	Dye type	Dye Carbon number	Modifying agent	Modifying technique	Applied pressure	Membrane flux	Dye removal	Ref
NF	PSF	Anionic (MB)	37	TEOA-TMC-PAA	Interfacial polymerization and physio-chemical	5 bar	40.25 LMH	99.6%	70
TFN	HPAN	Anionic (CR, MB, reactive black5, Direct red 23)	32 37 26 35	PVP-uio-66-NH_2-PVA-GA	Drop coating	4 bar	52.36 LMH	99.89-100%	71
NF	HPAN	Anionic (CR, MB) Cationic(MB)	32 37 16	Sulfonated Dopamine(SDA)	Interfacial polymerization	6 bar	62.2 LMH	99.9%	72
Composite	PES	Anionic(Reactive black 5, Reactive Green 19)	26 40	MOS_2-PSBMA	MMM(Phase inversion)	6 bar	108.3 LMH	98.2% 99.3%	73
Loose NF	HPAN	Anionic(CR, MB)	32 37	PEI-GA	Dip Coating	2 bar	51 LMH	97.1% 97.3%	74
Loose NF	PVDF	Anionic(CR)	32	PAA	UV-grafting	4 bar	104 LMH	99.38	75
Composite	PAN	Anionic (CR, Reactive-black-5, reactive orange16	32 26 20	PDA-PEI/TiO_2 -Ag	Coating and vacuum filtration	2 bar	81.2 LMH	99.6% 99.5% 96.2%	76
Loose NF	PES	Anionic (CR) Cationic (MB)	32 37	MOF-SBMA/PDA	Coating and surface functionalization	1.5 bar	63 LMH	99.9%	This work

Table 3: A comparison of the performance of various surface modified membranes developed for dye removal reported in literature.

Conclusion

In this study, in-situ heterogeneous nucleation and growth of ZIF-7 nano-crystals (MOF) was developed on the functional sites of PDA-assisted coating. Also, the SBMA zwitterion was co-deposited with PDA through the aza-Michael reaction to obtain a dense layer with high dye rejection capability. The zwitterion incorporation into PDA matrix played a favorable role in the performance improvement of the membrane also in terms of ZIF-7 formation and resulting surface density. The results indicated that MOF-SBMA/PDA membrane provided suitable water flux and high dye retention for loose nanofiltration applications. Perhaps most importantly, the membrane demonstrated remarkable antifouling properties due to the presence of hydrophilic SBMA zwitterion. Considering the adaptable surface modification, this functionalization strategy exploiting the aza-Michael addition offers a platform for developing diverse surface modified membranes with promising potential for industrial applications necessitating the separation of aqueous streams from low molecular weight compounds.

References

1. Firouzjaei, M. D.; Afkhami, F. A.; Esfahani, M. R.; Turner, C. H.; Nejati, S., Experimental and molecular dynamics study on dye removal from water by a graphene oxide-copper-metal organic framework nanocomposite. *Journal of Water Process Engineering* **2020,** *34*, 101180.

2. Quah, B. J.; Warren, H. S.; Parish, C. R., Monitoring lymphocyte proliferation in vitro and in vivo with the intracellular fluorescent dye carboxyfluorescein diacetate succinimidyl ester. *Nature protocols* **2007,** *2*, (9), 2049-2056.

3. Zhang, R.; Liu, Y.; He, M.; Su, Y.; Zhao, X.; Elimelech, M.; Jiang, Z., Antifouling membranes for sustainable water purification: strategies and mechanisms. *Chemical Society Reviews* **2016,** *45*, (21), 5888-5924.

4. Firouzjaei, M. D.; Seyedpour, S. F.; Aktij, S. A.; Giagnorio, M.; Bazrafshan, N.; Mollahosseini, A.; Samadi, F.; Ahmadalipour, S.; Firouzjaei, F. D.; Esfahani, M. R., Recent advances in functionalized polymer membranes for biofouling control and mitigation in forward osmosis. *Journal of Membrane Science* **2020,** *596*, 117604.

5. Esfahani, M. R.; Aktij, S. A.; Dabaghian, Z.; Firouzjaei, M. D.; Rahimpour, A.; Eke, J.; Escobar, I. C.; Abolhassani, M.; Greenlee, L. F.; Esfahani, A. R., Nanocomposite membranes for water separation and purification: Fabrication, modification, and applications. *Separation and Purification Technology* **2019,** *213*, 465-499.

6. Capozzi, L. C.; Mehmood, F. M.; Giagnorio, M.; Tiraferri, A.; Cerruti, M.; Sangermano, M., Ultrafiltration membranes functionalized with polydopamine with enhanced contaminant removal by adsorption. *Macromolecular Materials and Engineering* **2017,** *302*, (5), 1600481.

7. Kim, H. W.; McCloskey, B. D.; Choi, T. H.; Lee, C.; Kim, M.-J.; Freeman, B. D.; Park, H. B., Oxygen concentration control of dopamine-induced high uniformity surface coating chemistry. *ACS applied materials & interfaces* **2013,** *5*, (2), 233-238.

8. Ye, Q.; Zhou, F.; Liu, W., Bioinspired catecholic chemistry for surface modification. *Chemical Society Reviews* **2011,** *40*, (7), 4244-4258.

9. Yeon, D. K.; Ko, S.; Jeong, S.; Hong, S.-P.; Kang, S. M.; Cho, W. K., Oxidation-mediated, zwitterionic polydopamine coatings for marine antifouling applications. *Langmuir* **2018,** *35*, (5), 1227-1234.

10. Wang, Z.; Wang, Z.; Lin, S.; Jin, H.; Gao, S.; Zhu, Y.; Jin, J., Nanoparticle-templated nanofiltration membranes for ultrahigh performance desalination. *Nature communications* **2018,** *9*, (1), 1-9.

11. Pejman, M.; Firouzjaei, M. D.; Aktij, S. A.; Das, P.; Zolghadr, E.; Jafarian, H.; Shamsabadi, A. A.; Elliott, M.; Esfahani, M. R.; Sangermano, M.; Sadrzadeh, M.; Wujcik, E. K.; Rahimpour, A.; Tiraferri, A., Improved antifouling and antibacterial properties of forward osmosis membranes through surface modification with zwitterions and silver-based metal organic frameworks. *Journal of Membrane Science* **2020,** *611*, 118352.

12. Pejman, M.; Dadashi Firouzjaei, M.; Aghapour Aktij, S.; Das, P.; Zolghadr, E.; Jafarian, H.; Arabi Shamsabadi, A.; Elliott, M.; Sadrzadeh, M.; Sangermano, M.; Rahimpour, A.; Tiraferri, A., In Situ Ag-MOF Growth on Pre-Grafted Zwitterions Imparts Outstanding Antifouling Properties to Forward Osmosis Membranes. *ACS Applied Materials & Interfaces* **2020,** *12*, (32), 36287-36300.

13. Chao, S.; Li, X.; Li, Y.; Wang, Y.; Wang, C., Preparation of polydopamine-modified zeolitic imidazolate framework-8 functionalized electrospun fibers for efficient removal of tetracycline. *Journal of colloid and interface science* **2019,** *552*, 506-516.

14. Rahimpour, A.; Seyedpour, S. F.; Aghapour Aktij, S.; Dadashi Firouzjaei, M.; Zirehpour, A.; Arabi Shamsabadi, A.; Khoshhal Salestan, S.; Jabbari, M.; Soroush, M., Simultaneous Improvement of Antimicrobial, Antifouling, and Transport Properties of Forward Osmosis Membranes with Immobilized Highly-Compatible Polyrhodanine Nanoparticles. *Environ. Sci. Technol.* **2018**.

15. Zirehpour, A.; Rahimpour, A.; Arabi Shamsabadi, A.; Sharifian Gh, M.; Soroush, M., Mitigation of Thin-Film Composite Membrane Biofouling via Immobilizing Nano-Sized Biocidal Reservoirs in the Membrane Active Layer. *Environ. Sci. Technol.* **2017,** *51*, (10), 5511-5522.

16. Tiraferri, A.; Kang, Y.; Giannelis, E. P.; Elimelech, M., Superhydrophilic thin-film composite forward osmosis membranes for organic fouling control: fouling behavior and antifouling mechanisms. *Environmental science & technology* **2012,** *46*, (20), 11135-11144.

17. Liu, C.-Y.; Huang, C.-J., Functionalization of polydopamine via the aza-michael reaction for antimicrobial interfaces. *Langmuir* **2016,** *32*, (19), 5019-5028.

18. Yu, B.; Ye, G.; Chen, J.; Ma, S., Membrane-supported 1D MOF hollow superstructure array prepared by polydopamine-regulated contra-diffusion synthesis for uranium entrapment. *Environmental pollution* **2019,** *253*, 39-48.

19. Lee, H.; Dellatore, S. M.; Miller, W. M.; Messersmith, P. B., Mussel-inspired surface chemistry for multifunctional coatings. *science* **2007,** *318*, (5849), 426-430.

20. Ren, J.; Han, P.; Wei, H.; Jia, L., Fouling-resistant behavior of silver nanoparticle-modified surfaces against the bioadhesion of microalgae. *ACS applied materials & interfaces* **2014,** *6*, (6), 3829-3838.

21. Ryu, J.; Ku, S. H.; Lee, H.; Park, C. B., Mussel-inspired polydopamine coating as a universal route to hydroxyapatite crystallization. *Advanced Functional Materials* **2010,** *20*, (13), 2132-2139.

22. Yah, W. O.; Xu, H.; Soejima, H.; Ma, W.; Lvov, Y.; Takahara, A., Biomimetic dopamine derivative for selective polymer modification of halloysite nanotube lumen. *Journal of the American Chemical Society* **2012,** *134*, (29), 12134-12137.

23. Lee, M.; Ku, S. H.; Ryu, J.; Park, C. B., Mussel-inspired functionalization of carbon nanotubes for hydroxyapatite mineralization. *Journal of Materials Chemistry* **2010,** *20*, (40), 8848-8853.

24. Zhu, J.; Yuan, S.; Uliana, A.; Hou, J.; Li, J.; Li, X.; Tian, M.; Chen, Y.; Volodin, A.; Van der Bruggen, B., High-flux thin film composite membranes for nanofiltration mediated by a rapid co-deposition of polydopamine/piperazine. *Journal of Membrane Science* **2018,** *554*, 97-108.

25. Ruan, X.; Zhang, X.; Zhou, Z.; Jiang, X.; Dai, Y.; Yan, X.; He, G., ZIF-8 heterogeneous nucleation and growth mechanism on Zn (II)-doped polydopamine for composite membrane fabrication. *Separation and Purification Technology* **2019,** *214*, 95-103.

26. Hu, R.; Li, G.; Jiang, Y.; Zhang, Y.; Zou, J.-J.; Wang, L.; Zhang, X., Silver–zwitterion organic–inorganic nanocomposite with antimicrobial and antiadhesive capabilities. *Langmuir* **2013,** *29*, (11), 3773-3779.

27. Liu, Z.; Hu, Y., Sustainable antibiofouling properties of thin film composite forward osmosis membrane with rechargeable silver nanoparticles loading. *ACS applied materials & interfaces* **2016,** *8*, (33), 21666-21673.

28. Seyedpour, S. F.; Rahimpour, A.; Najafpour, G., Facile in-situ assembly of silver-based MOFs to surface functionalization of TFC membrane: A novel approach toward long-lasting biofouling mitigation. *Journal of Membrane Science* **2019,** *573*, 257-269.

29. Wei, X.; Wang, Z.; Wang, J.; Wang, S., A novel method of surface modification to polysulfone ultrafiltration membrane by preadsorption of citric acid or sodium bisulfite. *Memb. Water Treat* **2012,** *3*, 35-49.

30. Ghanbari, M.; Emadzadeh, D.; Lau, W.; Matsuura, T.; Ismail, A., Synthesis and characterization of novel thin film nanocomposite reverse osmosis membranes with improved organic fouling properties for water desalination. *Rsc Advances* **2015,** *5*, (27), 21268-21276.

31. Rahimpour, A.; Jahanshahi, M.; Mollahosseini, A.; Rajaeian, B., Structural and performance properties of UV-assisted TiO 2 deposited nano-composite PVDF/SPES membranes. *Desalination* **2012,** *285*, 31-38.

32. Van Assche, T. R.; Duerinck, T.; Gutierrez Sevillano, J. J.; Calero, S.; Baron, G. V.; Denayer, J. F., High adsorption capacities and two-step adsorption of polar adsorbates on copper–benzene-1, 3, 5-tricarboxylate metal–organic framework. *The Journal of Physical Chemistry C* **2013,** *117*, (35), 18100-18111.

33. Zhao, Y.-T.; Yu, L.-Q.; Xia, X.; Yang, X.-Y.; Hu, W.; Lv, Y.-K., Evaluation of the adsorption and desorption properties of zeolitic imidazolate framework-7 for volatile organic compounds through thermal desorption-gas chromatography. *Analytical Methods* **2018,** *10*, (40), 4894-4901.

34. Seyedpour, S. F.; Arabi Shamsabadi, A.; Khoshhal Salestan, S.; Dadashi Firouzjaei, M.; Sharifian Gh, M.; Rahimpour, A.; Akbari Afkhami, F.; Shirzad Kebria, M. r.; Elliott, M. A.; Tiraferri, A., Tailoring the Biocidal Activity of Novel Silver-Based Metal Azolate Frameworks. *ACS Sustainable Chem. Eng.* **2020**.

35. Kołodziejczak-Radzimska, A.; Markiewicz, E.; Jesionowski, T., Structural characterisation of ZnO particles obtained by the emulsion precipitation method. *Journal of Nanomaterials* **2012,** *2012*.

36. Hou, J.; Sutrisna, P. D.; Wang, T.; Gao, S.; Li, Q.; Zhou, C.; Sun, S.; Yang, H.-C.; Wei, F.; Ruggiero, M. T., Unraveling the interfacial structure–performance correlation of flexible metal–organic framework membranes on polymeric substrates. *ACS applied materials & interfaces* **2019,** *11*, (5), 5570-5577.

37. Xing, J.; Wang, Q.; He, T.; Zhou, Z.; Chen, D.; Yi, X.; Wang, Z.; Wang, R.; Tan, G.; Yu, P., Polydopamine-Assisted Immobilization of Copper Ions onto Hemodialysis Membranes for Antimicrobial. *ACS Applied Bio Materials* **2018,** *1*, (5), 1236-1243.

38. Li, M.; Sun, P.; Wu, Q.; Liu, D.; Zhou, L., Core–shell magnetic metal–organic framework molecularly imprinted nanospheres for specific adsorption of tetrabromobisphenol A from water. *Environmental Science: Nano* **2018,** *5*, (11), 2651-2662.

39. Ang, H.; Hong, L., Polycationic polymer-regulated assembling of 2D MOF nanosheets for high-performance nanofiltration. *ACS applied materials & interfaces* **2017,** *9*, (33), 28079-28088.

40. Shahkaramipour, N.; Ramanan, S. N.; Fister, D.; Park, E.; Venna, S. R.; Sun, H.; Cheng, C.; Lin, H., Facile grafting of zwitterions onto the membrane surface to enhance

antifouling properties for wastewater reuse. *Industrial & Engineering Chemistry Research* **2017,** *56*, (32), 9202-9212.

41. Chen, K.; Xie, K.; Long, Q.; Deng, L.; Fu, Z.; Xiao, H.; Xie, L., Fabrication of core–shell Ag@ pDA@ HAp nanoparticles with the ability for controlled release of Ag+ and superior hemocompatibility. *Rsc Advances* **2017,** *7*, (47), 29368-29377.

42. Kundu, S.; Malik, B.; Pattanayak, D. K.; Pillai, V. K., Effect of Dimensionality and Doping in Quasi-"One-Dimensional (1-D)" Nitrogen-Doped Graphene Nanoribbons on the Oxygen Reduction Reaction. *ACS applied materials & interfaces* **2017,** *9*, (44), 38409-38418.

43. Li, Y.; Cai, X.; Chen, S.; Zhang, H.; Zhang, K. H.; Hong, J.; Chen, B.; Kuo, D. H.; Wang, W., Highly Dispersed Metal Carbide on ZIF-Derived Pyridinic-N-Doped Carbon for CO2 Enrichment and Selective Hydrogenation. *ChemSusChem* **2018,** *11*, (6), 1040-1047.

44. Mozafari, M.; Seyedpour, S. F.; Salestan, S. K.; Rahimpour, A.; Shamsabadi, A. A.; Firouzjaei, M. D.; Esfahani, M. R.; Tiraferri, A.; Mohsenian, H.; Sangermano, M., Facile Cu-BTC surface modification of thin chitosan film coated polyethersulfone membranes with improved antifouling properties for sustainable removal of manganese. *Journal of Membrane Science* **2019**, 117200.

45. Tang, C. Y.; Kwon, Y.-N.; Leckie, J. O., Effect of membrane chemistry and coating layer on physiochemical properties of thin film composite polyamide RO and NF membranes: II. Membrane physiochemical properties and their dependence on polyamide and coating layers. *Desalination* **2009,** *242*, (1-3), 168-182.

46. Xia, S.; Yao, L.; Zhao, Y.; Li, N.; Zheng, Y., Preparation of graphene oxide modified polyamide thin film composite membranes with improved hydrophilicity for natural organic matter removal. *Chemical Engineering Journal* **2015,** *280*, 720-727.

47. Kang, G.-d.; Cao, Y.-m. J. W. r., Development of antifouling reverse osmosis membranes for water treatment: a review. **2012,** *46*, (3), 584-600.

48. Asadollahi, M.; Bastani, D.; Musavi, S. A., Enhancement of surface properties and performance of reverse osmosis membranes after surface modification: a review. *Desalination* **2017,** *420*, 330-383.

49. Van der Bruggen, B.; Mänttäri, M.; Nyström, M., Drawbacks of applying nanofiltration and how to avoid them: a review. *Separation and purification technology* **2008,** *63*, (2), 251-263.

50. Al-Amoudi, A.; Lovitt, R. W., Fouling strategies and the cleaning system of NF membranes and factors affecting cleaning efficiency. *Journal of Membrane Science* **2007,** *303*, (1-2), 4-28.

51. Liu, J.; Xu, H.; Tang, X.; Xu, J.; Jin, Z.; Li, H.; Wang, S.; Gou, J.; Jin, X., Simple and tunable surface coatings via polydopamine for modulating pharmacokinetics, cell uptake and biodistribution of polymeric nanoparticles. *Rsc Advances* **2017,** *7*, (26), 15864-15876.

52. Tejido-Rastrilla, R.; Ferraris, S.; Goldmann, W. H.; Grünewald, A.; Detsch, R.; Baldi, G.; Spriano, S.; Boccaccini, A. R., Studies on cell compatibility, antibacterial behavior, and zeta potential of Ag-containing polydopamine-coated bioactive glass-ceramic. *Materials* **2019,** *12*, (3), 500.

53. Zhu, J.; Tian, M.; Hou, J.; Wang, J.; Lin, J.; Zhang, Y.; Liu, J.; Van der Bruggen, B., Surface zwitterionic functionalized graphene oxide for a novel loose nanofiltration membrane. *Journal of Materials Chemistry A* **2016,** *4*, (5), 1980-1990.

54. Bryers, J. D., Biofilms and the technological implications of microbial cell adhesion. *Colloids and Surfaces B: Biointerfaces* **1994,** *2*, (1-3), 9-23.

55. Novak, S.; Maver, U.; Peternel, Š.; Venturini, P.; Bele, M.; Gaberšček, M., Electrophoretic deposition as a tool for separation of protein inclusion bodies from host bacteria in suspension. *Colloids and Surfaces A: Physicochemical and Engineering Aspects* **2009,** *340*, (1-3), 155-160.

56. Schwegmann, H.; Feitz, A. J.; Frimmel, F. H., Influence of the zeta potential on the sorption and toxicity of iron oxide nanoparticles on S. cerevisiae and E. coli. *Journal of colloid and interface science* **2010,** *347*, (1), 43-48.

57. Firouzjaei, M. D.; Shamsabadi, A. A.; Aktij, S. A.; Seyedpour, S. F.; Sharifian Gh, M.; Rahimpour, A.; Esfahani, M. R.; Ulbricht, M.; Soroush, M., Exploiting Synergetic Effects of Graphene Oxide and a Silver-Based Metal–Organic Framework To Enhance Antifouling and Anti-Biofouling Properties of Thin-Film Nanocomposite Membranes. *ACS applied materials & interfaces* **2018,** *10*, (49), 42967-42978.

58. Li, J.; Gong, J.-L.; Zeng, G.-M.; Zhang, P.; Song, B.; Cao, W.-C.; Fang, S.-Y.; Huan, S.-Y.; Ye, J., The performance of UiO-66-NH2/graphene oxide (GO) composite membrane for removal of differently charged mixed dyes. *Chemosphere* **2019,** *237*, 124517.

59. Fu, J.; Chen, Z.; Wang, M.; Liu, S.; Zhang, J.; Zhang, J.; Han, R.; Xu, Q., Adsorption of methylene blue by a high-efficiency adsorbent (polydopamine microspheres): kinetics, isotherm, thermodynamics and mechanism analysis. *Chemical Engineering Journal* **2015,** *259*, 53-61.

60. Kadhom, M.; Albayati, N.; Alalwan, H.; Al-Furaiji, M., Removal of dyes by agricultural waste. *Sustainable Chemistry and Pharmacy* **2020,** *16*, 100259.

61. Krishnan, S.; Weinman, C. J.; Ober, C. K., Advances in polymers for anti-biofouling surfaces. *Journal of Materials Chemistry* **2008,** *18*, (29), 3405-3413.

62. Shen, L.; Zhang, X.; Zuo, J.; Wang, Y., Performance enhancement of TFC FO membranes with polyethyleneimine modification and post-treatment. *J Memb Sci.* **2017,** *534*, 46-58.

63. Azari, S.; Zou, L., Using zwitterionic amino acid l-DOPA to modify the surface of thin film composite polyamide reverse osmosis membranes to increase their fouling resistance. *Journal of membrane science* **2012,** *401*, 68-75.

64. Kasemset, S.; Lee, A.; Miller, D. J.; Freeman, B. D.; Sharma, M. M., Effect of polydopamine deposition conditions on fouling resistance, physical properties, and permeation properties of reverse osmosis membranes in oil/water separation. *Journal of membrane science* **2013,** *425*, 208-216.

65. Ye, G.; Lee, J.; Perreault, F. o.; Elimelech, M., Controlled architecture of dual-functional block copolymer brushes on thin-film composite membranes for integrated "defending" and "attacking" strategies against biofouling. *ACS Appl. Mater. Interfaces* **2015,** *7*, (41), 23069-23079.

66. Tirado, M. L. M.; Bass, M.; Piatkovsky, M.; Ulbricht, M.; Herzberg, M.; Freger, V., Assessing biofouling resistance of a polyamide reverse osmosis membrane surface-modified with a zwitterionic polymer. *Journal of Membrane Science* **2016,** *520*, 490-498.

67. Zhang, Y.; Le Li, J.; Cai, T.; Cheng, Z. L.; Li, X.; Chung, T.-S., Sulfonated hyperbranched polyglycerol grafted membranes with antifouling properties for sustainable osmotic power generation using municipal wastewater. *Journal of membrane science* **2018,** *563*, 521-530.

68. Liu, C.; Faria, A. F.; Ma, J.; Elimelech, M., Mitigation of Biofilm Development on Thin-Film Composite Membranes Functionalized with Zwitterionic Polymers and Silver Nanoparticles. *Environ. Sci. Technol.* **2016,** *51*, (1), 182-191.

69. Choudhury, R. R.; Gohil, J. M.; Mohanty, S.; Nayak, S. K., Antifouling, fouling release and antimicrobial materials for surface modification of reverse osmosis and nanofiltration membranes. *Journal of Materials Chemistry A* **2018,** *6*, (2), 313-333.

70. Wu, Y.; Gao, M.; Chen, W.; Lü, Z.; Yu, S.; Liu, M.; Gao, C., Efficient removal of anionic dye by constructing thin-film composite membrane with high perm-selectivity and improved anti-dye-deposition property. *Desalination* **2020,** *476*, 114228.

71. Zhao, P.; Li, R.; Wu, W.; Wang, J.; Liu, J.; Zhang, Y., In-situ growth of polyvinylpyrrolidone modified Zr-MOFs thin-film nanocomposite (TFN) for efficient dyes removal. *Composites Part B: Engineering* **2019,** *176*, 107208.

72. Ding, J.; Wu, H.; Wu, P., Development of nanofiltration membranes using mussel-inspired sulfonated dopamine for interfacial polymerization. *Journal of Membrane Science* **2020,** *598*, 117658.

73. Liang, X.; Wang, P.; Wang, J.; Zhang, Y.; Wu, W.; Liu, J.; Van der Bruggen, B., Zwitterionic functionalized MoS2 nanosheets for a novel composite membrane with effective salt/dye separation performance. *Journal of Membrane Science* **2019,** *573*, 270-279.

74. Zhao, S.; Wang, Z., A loose nano-filtration membrane prepared by coating HPAN UF membrane with modified PEI for dye reuse and desalination. *Journal of membrane science* **2017,** *524*, 214-224.

75. Chiao, Y.-H.; Chen, S.-T.; Yap Ang, M. B. M.; Patra, T.; Castilla-Casadiego, D. A.; Fan, R.; Almodovar, J.; Hung, W.-S.; Wickramasinghe, S. R., High-Performance Polyacrylic Acid-Grafted PVDF Nanofiltration Membrane with Good Antifouling Property for the Textile Industry. *Polymers* **2020,** *12*, (11), 2443.

76. Li, J.; Yuan, S.; Zhu, J.; Van der Bruggen, B., High-flux, antibacterial composite membranes via polydopamine-assisted PEI-TiO2/Ag modification for dye removal. *Chemical Engineering Journal* **2019,** *373*, 275-284.